

Propagation Properties of Leaky SAW on Water-loaded LiTaO₃/Quartz Bonded Structure

水負荷 LiTaO₃/水晶接合構造上の漏洩弾性表面波の伝搬特性

Shoji Kakio¹, Yoshiki Kato¹, Ryota Suenaga¹, Masashi Suzuki¹, Ami Tezuka², Hiroyuki Kuwae², Hiroaki Yokota³, Toshifumi Yonai³, Kazuhito Kishida³, and Jun Mizuno² (¹Univ. of Yamanashi; ²Waseda Univ.; ³The Japan Steel Works, Ltd.)
垣尾 省司¹, 加藤 良基¹, 末永 凌大¹, 鈴木 雅視¹, 手塚 彩水², 桑江 博之², 横田 裕章³, 米内 敏文³, 岸田 和人³, 水野 潤² (山梨大学,²早稲田大学,³日本製鋼所)

1. Introduction

For next-generation mobile communication systems, high-performance surface acoustic wave (SAW) devices are required. Recently, an “incredible high-performance SAW resonator” with a large Q factor and a small temperature coefficient of frequency (TCF) for a shear horizontal-type SAW (SH-SAW) has been reported, the structure of which is a combination of LiTaO₃ (LT), aluminum nitride (AlN), and SiO₂ thin films.¹ Moreover, a “hetero acoustic layer (HAL) SAW device” with a wide fractional bandwidth and a large impedance ratio for SH-SAWs,² and a high-frequency longitudinal leaky SAW (LLSAW) resonator with a LiNbO₃ (LN) thin plate and a multilayered acoustic reflector comprising a SiO₂/Pt layer³ have been reported. The authors have reported that, in a bonded structure comprising a quartz substrate and an LT or LN thin plate with a thickness less than one wavelengths, a large electromechanical coupling factor (K^2) and a small TCF for SH-SAWs and LLSAWs can be obtained simultaneously.⁴⁻⁶ However, differences between the measured and theoretical values of the resonance Q and TCF were observed owing to the inhomogeneity of the bond strength.

On the other hand, a line-focus-beam ultrasonic material characterization (LFB-UMC) system is suitable for highly accurate, nondestructive, and noncontact measurement of the elastic properties of materials.⁷ It provides the velocity and normalized attenuation factor of leaky surface acoustic waves (LSAWs) excited on a water-loaded material surface. The normalized attenuation factor includes leakage loss into water. We previously reported the possibility of evaluating acoustical loss from the difference between the measured and calculated normalized attenuation of LSAWs.^{8,9}

In this study, using an LFB-UMC system, we investigated the velocity and normalized attenuation factor of LSAWs on a water-loaded LT/quartz bonded structure.

2. Theoretical Calculation

The calculated phase velocity and normalized attenuation factor of LSAWs on water-loaded 36°YX

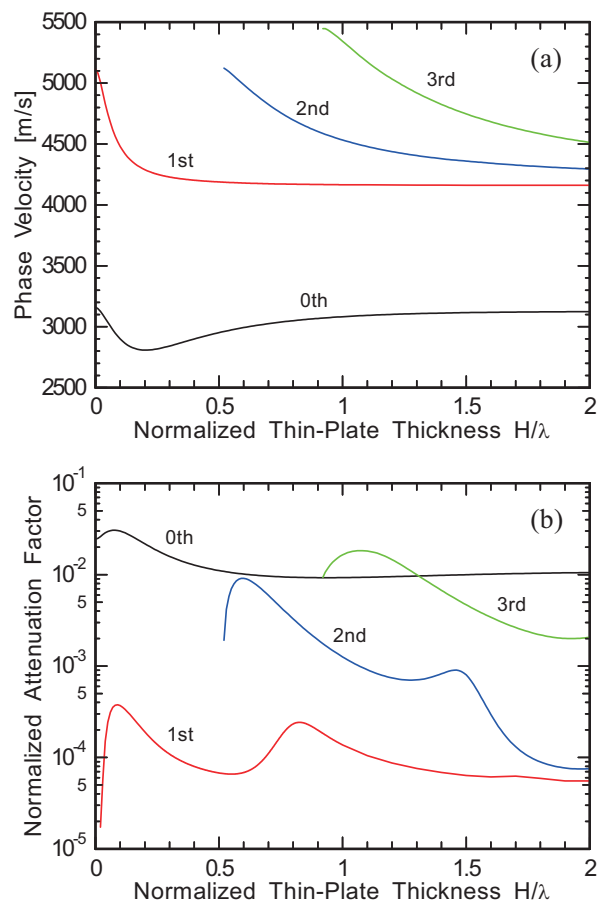


Fig. 1 Calculated dispersion curves of water-loaded 36°YX-LT/AT0°X-quartz: (a) phase velocity and (b) normalized attenuation factor.

-LT/AT0°X-quartz as a function of the LT thin-plate thickness normalized by the wavelength (H/λ) are shown in **Figs. 1(a) and 1(b)**, respectively. The number of propagation modes increases with increasing H/λ . The 0th and 1st modes correspond to the Rayleigh-type SAW and SH-SAW on the air/LT/quartz structure, respectively, and the 2nd and 3rd modes correspond to the higher modes of the SH-SAW. The phase velocity of the modes higher than the 1st mode monotonically decreases with increasing H/λ and converges to the value on single LT. On the other hand, the phase velocity of the 0th mode becomes lower than that on a single

LT at around $H/\lambda=0.2$. Such phenomena have been observed on an air/LT/quartz structure for an LLSAW.^{4,6}

As shown in Fig. 1(b), the higher modes have a smaller attenuation factor than that of the 0th mode. Therefore, the higher modes are considered to be useful for evaluating acoustical loss due to inhomogeneity of the bond strength. Unfortunately, in the measurement described in the next section, no propagation modes other than the 0th mode were observed.

3. Measured Propagation Properties

We prepared two samples of $36^\circ\text{YX-LT/AT}0^\circ\text{X}$ -quartz with LT thin-plate thicknesses H of $2.2\ \mu\text{m}$ and $6.3\ \mu\text{m}$ by the surface-activated room-temperature bonding technique.

The phase velocity and normalized attenuation factor of the 0th LSAW on these samples were measured using the LFB-UMC system in the frequency range from 100 to 300 MHz. The measured phase velocity and normalized attenuation factor are shown in Figs. 2(a) and 2(b), respectively, as a function of the product of the frequency f and H , together with the calculated values. The propagation directions in the measurement were 0°X and 90°X .

As shown in Fig. 2(a), the measured phase velocity of the LSAW was in good agreement with the calculated value for both cases. Moreover, the phenomenon in which the phase velocity of the 0th mode became lower than that on a single LT was observed experimentally. From Fig. 2(b), at $fH=600\text{--}1,200$ for the 90°X propagation of the sample of $H=6.3\ \mu\text{m}$, the measured normalized attenuation factor was slightly larger than the calculated value. However, it was judged that acoustical loss due to inhomogeneity of the bond strength was not observed in the measured frequency range because the measurements for the 90°X propagation in the fH range other than $600\text{--}1,200$ and for the 0°X propagation were in good agreement with the calculated values.

4. Conclusions

The phase velocity and normalized attenuation factor of the 0th LSAW on a water-loaded $36^\circ\text{YX-LT/AT}0^\circ\text{X}$ -quartz bonded structure were measured using an LFB-UMC system and were in good agreement with the calculated values for both the 0°X and 90°X propagation directions.

Acknowledgments

The authors thank Prof. J. Kushibiki, Dr. M. Arakawa, and Dr. Y. Ohashi of Tohoku University for their kind instructions on the LFB-UMC system. This work was supported by JSPS Grant-in-Aid for Scientific Research (B) no. 17H03233.

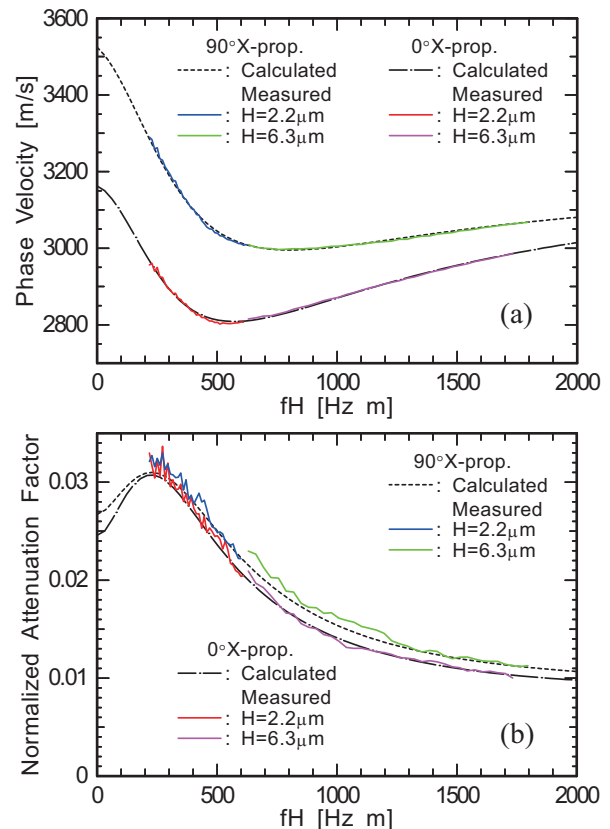


Fig. 2 Measured and calculated dispersion curves of water-loaded $36^\circ\text{YX-LT/AT}0^\circ\text{X}$ -quartz for 0°X and 90°X propagation directions: (a) phase velocity and (b) normalized attenuation factor.

References

1. T. Takai, H. Iwamoto, Y. Takamine, H. Yamazaki, T. Fuyutsume, H. Kyoya, T. Nakao, H. Kando, M. Hiramoto, T. Toi, M. Koshino, and N. Nakajima, IEEE Trans. Ultrason. Ferroelectr. Freq. Control **64**, 1382, 2017.
2. M. Kadota and S. Tanaka, Jpn. J. Appl. Phys. **57**, 07LD12, 2018.
3. T. Kimura, Y. Kishimoto, M. Omura, and K. Hashimoto, Jpn. J. Appl. Phys. **57**, 07LD15, 2018.
4. M. Gomi, T. Kataoka, J. Hayashi, and S. Kakio, Jpn. J. Appl. Phys. **56**, 07JD13, 2017.
5. J. Hayashi, K. Yamaya, M. Suzuki, S. Kakio, H. Suzuki, T. Yonai, K. Kishida, and J. Mizuno, Jpn. J. Appl. Phys. **57**, 07LD21, 2018.
6. J. Hayashi, K. Yamaya, S. Asakawa, M. Suzuki, S. Kakio, H. Kuwae, T. Yonai, K. Kishida, and J. Mizuno, Jpn. J. Appl. Phys. **58**, SGGC12, 2019.
7. J. Kushibiki and N. Chubachi, IEEE Trans. Sonics Ultrason. **SU-32**, 189, 1985.
8. R. Suenaga, M. Suzuki, S. Kakio, Y. Ohashi, M. Arakawa, and J. Kushibiki, Jpn. J. Appl. Phys. **57**, 07LC10, 2018.
9. R. Suenaga, M. Suzuki, S. Kakio, Y. Ohashi, M. Arakawa, and J. Kushibiki, Jpn. J. Appl. Phys. **58**, SGG A05, 2019.